Four-photon decay of orthopositronium: A test of charge-conjugation invariance

Jinfeng Yang, Masami Chiba, Ryosuke Hamatsu, Tachishige Hirose, Toshihiro Matsumoto, and Jie Yu*
Department of Physics, Tokyo Metropolitan University, 1-1 Minami Ohsawa, Hachioji-shi, Tokyo 192-03, Japan
(Received 26 January 1996)

Charge-conjugation (C) invariance demands that ortho- and parapositronium decay into an odd number and an even number of photons, respectively. For the test of the C invariance, we searched for a C-violating process, i.e., four-photon decay from orthopositronium, using a multi-γ-ray spectrometer. No C-violating process was observed leading to the upper limit as 2.6×10^{-6} at 90% confidence level for the branching ratio of four- to three-photon decays from orthopositronium. [S1050-2947(96)02909-5]

PACS number(s): 36.10.Dr, 12.20.Fv, 13.10.+q, 11.30.Er

I. INTRODUCTION

Positronium (Ps) is a bound state consisting of leptons only, i.e., an electron and a positron [1,2], and thus allows precision tests of quantum electrodynamics (QED) [3–6]. As a fermion-antifermion bound state, Ps has simple properties under the discrete symmetries of C, CP, and CPT transformations, where C denotes charge conjugation, P parity, and T time reversal. This offers us good opportunities to study the violation of these invariances [7–11].

Since Ps is an eigenstate of C, the C invariance imposes restrictions on the decay of Ps into photons, i.e., Ps$\rightarrow n\gamma$. The eigenvalue of C of n photons is $(-1)^n$ while that of Ps is $(-1)^{l+s}$, where l represents the relative orbital angular momentum and s the total spin. The C invariance thus gives rise to the relation of $(-1)^{l+s}=(-1)^n$. Since the eigenvalue of C is -1 for orthopositronium (o-Ps) and $+1$ for parapositronium (p-Ps), o-Ps and p-Ps should decay into an odd number and an even number of photons, respectively [1,2]. Therefore, the C violation can be studied for the process with $(-1)^{l+s}\neq(-1)^n$. Mills and Berko [9] investigated the three-photon annihilation of singlet state ($^1S_0\rightarrow3\gamma$) and obtained the upper limit of the branching ratio, $\lambda_{^1S_0\rightarrow3\gamma}/\lambda_{^1S_0\rightarrow2\gamma}$, as 2.8×10^{-6} for the 68% confidence level (CL). Mani and Rich [10] and Marko and Rich [11] performed experiments to search for C-violating four-photon decay of o-Ps (o-Ps$\rightarrow4\gamma$) using four NaI(Tl) counters placed at the corners of a tetrahedron. They obtained the upper limit of the branching ratio, $\lambda_{o\text{-Ps}\rightarrow4\gamma}/\lambda_{o\text{-Ps}\rightarrow3\gamma}$, as 8×10^{-6} for the 68% CL. The C invariance has also been investigated in hadron decays: the upper limits of C-violating π^0 and η decays were measured as $\lambda_{\pi^0\rightarrow3\gamma}/\lambda_{\text{total}}=3.1\times10^{-8}$ [12] and $\lambda_{\eta\rightarrow\pi^0\mu^+\mu^-}/\lambda_{\text{total}}=5\times10^{-6}$ [13] for the 90% CL, respectively. Although no C-violating processes were found in these experiments, it is important to study it with better sensitivity, since the C invariance is a principal discrete symmetry in fundamental processes.

In this paper, we present a precise measurement of the C-violating o-Ps$\rightarrow4\gamma$ process using a multi-γ-ray spectrometer (MGS) together with measurement of the C-invariant $^1S_0\rightarrow4\gamma$ process for the check of the experimental system. In Sec. II, we describe the experimental apparatus and data collection process in the experiment. Section III contains the data selection and event analysis. In Sec. IV, we present the detector performance and detection efficiency of the $^1S_0\rightarrow4\gamma$ process obtained by a Monte Carlo simulation. The estimation of backgrounds is also contained in this section. Section V is devoted to the results and conclusions.

II. EXPERIMENT

A. Experimental apparatus

In order to search for the o-Ps$\rightarrow4\gamma$ process, we employ a MGS [4] consisting of 32 NaI(Tl) scintillators with lead shields and photomultiplier tubes (PMT: Hamamatsu R1911, with a diameter of 3 in.). Each NaI(Tl) scintillator is placed on a surface of an icosidodecahedron. The size of the NaI(Tl) crystals is $76.2^{+0}_{-0.15}$ mm in diameter and $101.6^{+0.5}_{-1.0}$ mm in length. The front face of each NaI(Tl) scintillator is located at a distance of 261.6 ± 0.6 mm from the center of MGS covering a solid angle of $(0.521\pm0.005)\%$ of 4π sr. There are 16 couples of collinear NaI(Tl) scintillators, which are utilized for the measurement of two-photon decay of Ps. MGS also contains 15 planes including the origin of the MGS with eight NaI(Tl) scintillators, as shown in Fig. 1(a), which are utilized for the measurement of three-photon decay of Ps. The lead shields are designed to prevent Compton scattered photons in a NaI(Tl) scintillator from entering other NaI(Tl) scintillators except for backward scattering. A photon scattered in a NaI(Tl) scintillator must penetrate at least 30 mm of the lead shields to enter another NaI(Tl) scintillator. Hence we can achieve a suppression factor of 10^{-6} for Compton-scattered photons of 300 keV, which corresponds to the maximum energy of scattered photons when incident photons have a maximum energy of 511 keV. Signals from 32 PMT's are independently fed to discriminators, scalars, analog-to-digital converters (ADC's) and time-to-digital converters (TDC's) in the standard NIM and CAMAC systems. Data from ADC's, TDC's, and scalars are collected with a personal computer (NEC PC-H9801). The energy and time resolutions for the NaI(Tl) scintillators are expressed, respectively, as $\sigma_E(\text{keV})/E=(40.2/\sqrt{E}+1.9)\%$ and $\sigma_t(\text{ns})=34.0/(\sqrt{E}-6.5)-10.2/(E-38.0)$ (E in keV), resulting in $\sigma_E=19$ keV and $\sigma_t=2$–8 ns at the energy of 120–511 keV.

*Present address: The Institute of Japanese Union of Scientists and Engineers, Shibuya, Tokyo, Japan.

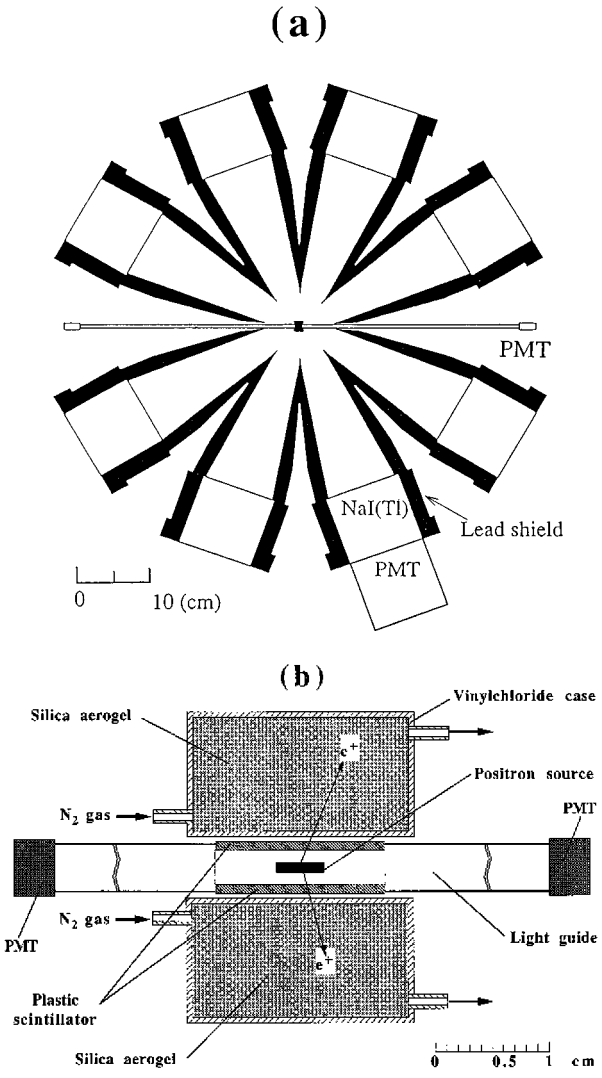

FIG. 1. (a) Cross section of the multi-γ-ray spectrometer (MGS). (b) Target region consisting of the positron source, the plastic scintillators, the light guides, and the silica aerogels contained in the hard-vinylchloride cases.

A target region at the center of the MGS contains a positron source, plastic scintillators, light guides, and silica aerogels, as shown in Fig. 1(b). The positron source, ^{68}Ge (73 kBq on average during the experiment) with a diameter of 4 mm, a thickness of 0.5 mm, and a density of 1.39 g/cm^3, is placed between two plastic scintillators (NE102A, with a dimension of $0.5\times10\times15$ mm^3). In the decay scheme, ^{68}Ge decays into ^{68}Ga only through orbital electron capture with a half-life of 288 days. Then ^{68}Ga decays into the ground state of ^{68}Zn with a branching fraction of 89% through β^+ decay whose maximum kinetic energy is 1889 keV. Transition photons with 1077 keV are emitted from the excited state of ^{68}Zn populated in the β^+ decay with a fraction of 1.3%. Positrons passing through the plastic scintillators radiate scintillation light, which is transmitted through two acrylic light guides (a dimension of $4\times10\times320$ mm^3) to two PMT's (Hamamatsu, R647) at both sides, as shown in Fig. 1. The coincidence of the signals from the two PMT's gives a trigger-counter signal with which one can get the number of positrons and a start signal of the TDC. The two pieces of the silica aerogel, produced by Gadelius Co. Ltd. with a density of 0.3 g/cm^3 and a dimension of $19\times10.6\times19$ mm^3, are enclosed with the two hard-vinylchloride cases attached outside the two plastic scintillators. The positrons losing their energies stop in the silica aerogels and form o-Ps. Sometimes, o-Ps collides with electrons of surrounding materials or unpaired electrons of oxygen in air, and annihilates into two photons on account of pick-off effect. In order to suppress this effect, we let N_2 gas flow continuously (50 ml/min) in the hard-vinylchloride cases.

B. Data collection

For the measurement of o-Ps$\rightarrow4\gamma$ events, the trigger conditions for the data taking to the personal computer are provided as follows: (a) any four hits of the NaI(Tl) scintillators should coincide in the time window from 0 to 400 ns, which begin at the trigger-counter signals; (b) events that contain the collinear hits are rejected. After applying these trigger conditions, the four-hit events of 515 602 are obtained during the data-taking period of 2.02×10^7 s.

We obtain the production rate of o-Ps as 0.132 ± 0.004 for positrons stopped in the silica aerogels by measuring the three-photon decay of o-Ps as described in Ref. [6]. The lifetime of o-Ps in the silica aerogels is measured to be 120.6 ± 2.0 ns. We also measure both three- and two-photon annihilations of free positrons and free electrons, and then obtain the branching ratio of three- to two-photon prompt annihilations as $(1.2\pm0.3)/372$ [6], which is consistent with the QED prediction of 1/372.

III. EVENT ANALYSIS

Although a large number of two-photon annihilation events are effectively suppressed in the trigger condition (b), many other backgrounds still remain in the four-hit events. Candidates of $e^+e^-\rightarrow4\gamma$ events are selected by applying the following criteria: (i) rejection of the four-hit events, which contain three hits in one of the 15 planes arising from the $e^+e^-\rightarrow3\gamma$ process; (ii) selection of each photon with the energy E_i, $120\leqslant E_i\leqslant450$ keV, to reject bremsstrahlung photons emitted from the positron and noncollinear two-photon annihilations in which one of the two photons scatters by Compton effect in the target region; (iii) selection of four photons emitted simultaneously with a residual time R_t shorter than 1.0, R_t being defined as $\sqrt{\frac{1}{4}\Sigma_{i=1}^4(t_i-\tau)^2/\sigma_{t_i}^2}$ where t_i represents the time interval between the trigger-counter signal and the NaI(Tl) hits, τ is a mean time among the four photons as $\tau=\Sigma_{i=1}^4(t_i/\sigma_{t_i}^2)/\Sigma_{i=1}^4(1/\sigma_{t_i}^2)$, and σ_{t_i} is a time resolution of the NaI(Tl) scintillators; (iv) selection of events based on the momentum conservation with $P=|\Sigma_{i=1}^4\vec{P}_i|\leqslant80$ keV/c and the energy conservation with $E=|\Sigma_{i=1}^4E_i-2m_e|\leqslant30$ keV, where $\vec{P}_i$ and m_e are the momentum vector of the ith photon and electron mass, respectively.

In each step of (i)–(iv), the number of collected events, 515 602, is reduced to (i) 312 768, (ii) 100 297, (iii) 12 107, and (iv) 40. We divide the events into those with $\tau\leqslant10$ ns and those with $\tau>10$ ns after applying the selection criteria (i)–(iv). The former consists of a p-Ps$\rightarrow4\gamma$ process and a free annihilation of singlet state, i.e., $^1S_0\rightarrow4\gamma$. The latter

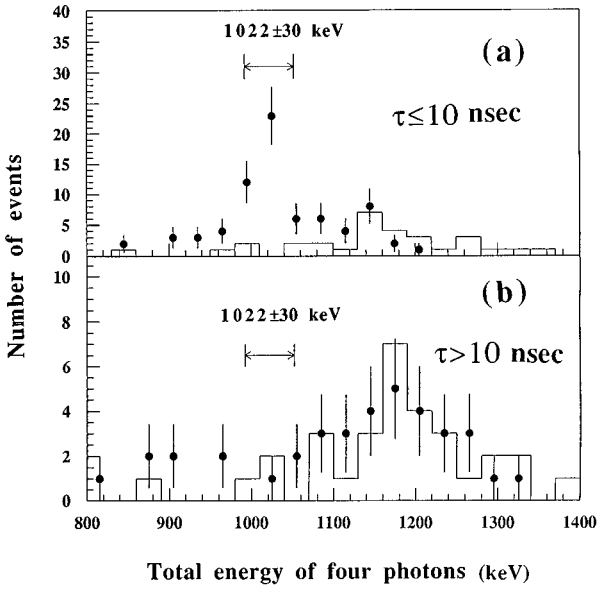

FIG. 2. Distribution of the total energy of four photons for (a) $\tau \leqslant 10$ ns and (b) $\tau > 10$ ns under the selection criteria (i)–(iii) (see in the text) and $P \leqslant 80$ keV/c. The histogram shows the backgrounds estimated from the simulation.

contains the o-Ps$\rightarrow 4\gamma$ process if the C violation takes place in the decay of o-Ps. Because of the short lifetime ($\sim$0.12 ns [1,2]) of p-Ps, the contamination of the p-Ps$\rightarrow 4\gamma$ process in the events with $\tau > 10$ ns is negligible. Among the 40 events, we observe 3 events with $\tau > 10$ ns as seen in Figs. 2(b) and 3(b).

IV. MONTE CARLO SIMULATION

A. Detector performance

In order to clarify the behavior of positrons and photons in the materials, we simulate the interaction process of positrons in MGS using a Monte Carlo program of the electron-gamma shower code (EGS4) [14]. In the simulation, we generate the events of $e^+e^- \rightarrow 3\gamma$ and 4γ based on QED using GRACE [15] and BASES/SPRING [16] codes.

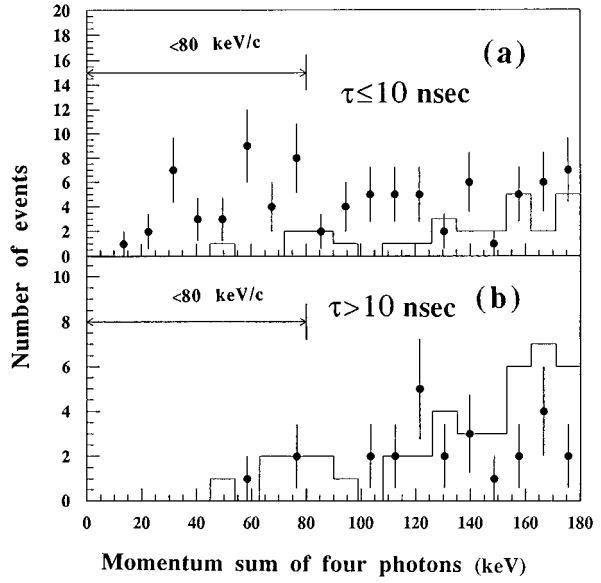

FIG. 3. Distribution of the momentum sum of four photons for (a) $\tau \leqslant 10$ ns and (b) $\tau > 10$ ns under the selection criteria (i)–(iii) (see in the text) and $E \leqslant 30$ keV. The histogram shows the backgrounds estimated from the simulation.

First of all, it is observed that positrons of 79.3% hit one of the two plastic scintillators to generate the trigger-counter signals; the others annihilate in the source material or escape from the gap between the two plastic scintillators. Furthermore the program clarifies detailed behaviors of the positrons after hitting the plastic scintillator as follows: (1) those of 31.9% stop in the silica aerogel, forming Ps or annihilating promptly; (2) those of 45.8% stop in the plastic scintillators and the hard-vinylchloride cases, and then mainly annihilate promptly; (3) the remaining 22.3% escapes from the silica aerogel. We also obtain the detection efficiency of the ${}^1S_0 \rightarrow 4\gamma$ process as $(3.3 \pm 0.7) \times 10^{-5}$ in MGS after applying the selection criteria (i)–(iv).

B. Estimation of backgrounds

Two types of backgrounds are considered in the analysis. The first type (Nos. 1–3 in Table I) for $\tau \leqslant 10$ ns is caused by an incident positron, which annihilates into three photons in association with the bremsstrahlung photon or the transition photon. Here, one of the photons in the three-photon annihilation is scattered by Compton scattering in the target region and accordingly cannot be rejected by the selection criterion (i). The second type (Nos. 4–20 in Table I) is due to accidental coincidence of two incident positrons. In the backgrounds of Nos. 4–6, the first positron hits the plastic scintillator and all annihilated photons are missed in the NaI scintillators. In the time window of 400 ns, the second positron annihilates promptly into three photons in association with the bremsstrahlung photon or the transition photon. These four photons are measured as an imitated event of the o-Ps$\rightarrow 4\gamma$ process. The three backgrounds (Nos. 4–6) cannot be rejected with the selection criterion (iii), since the start and stop signals in TDC are generated by the first positron and the photons annihilated from the second positron, respectively. Backgrounds of Nos. 7–20 are due to two incident positrons that annihilate into two different events with $R_t > 1.0$.

Using the simulation, we estimate the relative contributions of all backgrounds under the selection criteria (i)–(iv) as shown in Table I. After applying the selection criteria (i)–(iii), we plot the distribution of total energy of four photons for $P \leqslant 80$ keV/c in Fig. 2 and the distribution of the momentum sum of four photons for $E \leqslant 30$ keV in Fig. 3. The events of the ${}^1S_0 \rightarrow 4\gamma$ process are observed as the enhancements around 1022 keV in Fig. 2(a) and for $P \leqslant 80$ keV/c in Fig. 3(a). Figures 2(b) and 3(b) demonstrate that the events with $\tau > 10$ ns are consistent with the backgrounds. The enhancement around 1180 keV in Fig. 2(b) is caused by the background of No. 4 in Table I.

V. RESULTS AND CONCLUSIONS

After applying the selection criteria (i)–(iv), we obtain 37 events for the C invariant ${}^1S_0 \rightarrow 4\gamma$ process, which includes the background events of 2.0 ± 1.4(stat.) ± 0.1(syst.) estimated from the simulation as shown in Figs. 2(a) and 3(a). Then we obtain the branching ratio, $\lambda_{{}^1S_0 \rightarrow 4\gamma} / \lambda_{{}^1S_0 \rightarrow 2\gamma}$, as

TABLE I. Relative contributions of 20 different backgrounds in the experiment. The backgrounds due to one incident positron and two incident positrons are represented by the notations + and ×, respectively. The 2γ Compton and 3γ Compton mean two- and three-photon annihilations in which one of those photons is scattered in the target region by the Compton effect. The notation γ, γ_b, and γ_T represent annihilation, bremsstrahlung, and transition photons, respectively. The notation $\gamma_b(\gamma_b)$ represents two bremsstrahlung photons in which one photon in the parentheses is missed in the NaI(Tl) scintillators. The two- and three-photon annihilations are denoted as $\gamma(\gamma)$, $\gamma\gamma(\gamma)$, and $\gamma(\gamma\gamma)$ in which the photons in the parentheses are not detected. e^+ means that a positron passing through the target region hits a NaI(Tl) scintillator. (e^+) represents that a positron hits the plastic scintillator and all photons annihilated from this positron are missed in the NaI(Tl) scintillators.

No.	Background	Fraction (%)	
		$\tau \leqslant 10$ ns	$\tau > 10$ ns
1	3γ Compton$+\gamma_b$	79.9	
2	3γ Compton$+\gamma_T$	13.4	
3	3γ Compton$+\gamma_b(\gamma_b)$	5.8	
4	$(e^+)\times 3\gamma$ Compton$+\gamma_b$		55.2
5	$(e^+)\times 3\gamma$ Compton$+\gamma_T$		9.2
6	$(e^+)\times 3\gamma$ Compton$+\gamma_b(\gamma_b)$		4.0
7	3γ Compton$\times\gamma(\gamma)$	0.3	9.6
8	$\gamma\gamma(\gamma)\times\gamma\gamma(\gamma)$	0.2	6.8
9	3γ Compton$\times\gamma(\gamma\gamma)$	0.1	3.5
10	$\gamma\gamma(\gamma)\times 2\gamma$ Compton	0.1	3.1
11	3γ Compton$\times e^+$	0.07	2.3
12	3γ Compton$\times\gamma_b$	0.05	1.6
13	2γ Compton$\times 2\gamma$ Compton	0.02	
14	3γ Compton$\times\gamma_T$	0.008	0.3
15	3γ Compton$\times\gamma_b(\gamma_b)$	0.003	0.1
16	$\gamma\gamma(\gamma)\times(\gamma(\gamma)+\gamma_b)$	0.06	1.8
17	$\gamma\gamma(\gamma)\times(\gamma(\gamma\gamma)+\gamma_b)$	0.03	1.1
18	$\gamma\gamma(\gamma)\times(\gamma(\gamma)+\gamma_T)$	0.01	0.5
19	$\gamma\gamma(\gamma)\times(\gamma(\gamma\gamma)+\gamma_T)$	0.008	0.3
20	$\gamma\gamma(\gamma)\times(e^+ + \gamma_b)$	0.02	0.6

$[1.19\pm0.14(\text{stat.})\pm0.22(\text{syst.})]\times10^{-6}$, which is in good agreement with both the QED prediction, $(1.4796\pm0.0006)\times10^{-6}$ [4], and the previous experimental values, $[1.47\pm0.13(\text{stat.})\pm0.12(\text{syst.})]\times10^{-6}$ [4] and $[1.50\pm0.07(\text{stat.})\pm0.09(\text{syst.})]\times10^{-6}$ [5]. Therefore we conclude that our experimental system and the Monte Carlo simulation work well as expected.

In the measurement of the C-violating o-Ps$\rightarrow 4\gamma$ process, we obtain 3 events after applying the selection criteria (i)–(iv) as demonstrated in Figs. 2(b) and 3(b). The number of events agrees well with the number of backgrounds, $3.4\pm0.2(\text{stat.})\pm0.1(\text{syst.})$ estimated from the simulation. We derive the branching ratio $F^{4\gamma}$ as

$$F^{4\gamma}=\frac{\lambda_{o\text{-Ps}\rightarrow 4\gamma}}{\lambda_{o\text{-Ps}\rightarrow 3\gamma}}=\frac{N_{\text{expt}}-N_{\text{back}}}{N_{o\text{-Ps}}\epsilon^{4\gamma}_{o\text{-Ps}}}. \quad (1)$$

Here various quantities used are defined as follows: $N_{\text{expt}}=3$, the number of observed events; $N_{\text{back}}=3.4\pm0.2(\text{stat.})\pm0.1(\text{syst.})$, the number of estimated backgrounds; $N_{o\text{-Ps}}=(4.92\pm0.11)\times10^{10}$, the number of o-Ps formed in the silica aerogels; and $\epsilon^{4\gamma}_{o\text{-Ps}}=(3.3\pm0.7)\times10^{-5}$, the detection efficiency of the o-Ps$\rightarrow 4\gamma$ process. Since the 32 NaI(Tl) scintillators are arranged rather homogeneously on the surface of the MGS, it may be assumed that $\epsilon^{4\gamma}_{o\text{-Ps}}$ equals the detection efficiency of the ${}^1S_0\rightarrow 4\gamma$ process although the angular distribution of the photons for the o-Ps$\rightarrow 4\gamma$ process may be slightly different from that for the ${}^1S_0\rightarrow 4\gamma$ process. We then obtain

$$F^{4\gamma}=-[2.5\pm1.3(\text{stat.})\pm0.8(\text{syst.})]\times10^{-7}. \quad (2)$$

Hence we derive the upper limit $F^{4\gamma}_{\text{upper limit}}$ for the o-Ps$\rightarrow 4\gamma$ process under the assumption that the events are observed in a Poisson process that has two components, i.e., signal (N_{expt}) and background (N_{back}), as described in Ref. [17]:

$$F^{4\gamma}_{\text{upper limit}}=\begin{cases}1.5\times10^{-6} & \text{for } 68\% \text{ CL} \quad (3a)\\ 2.6\times10^{-6} & \text{for } 90\% \text{ CL} \quad (3b)\end{cases}$$

The upper limit for the 68% CL is improved by 5 times compared with the previous result of 8×10^{-6} for $\lambda_{(o\text{-Ps}\rightarrow 4\gamma)}/\lambda_{(o\text{-Ps}\rightarrow 3\gamma)}$ obtained in Ref. [11], and is also improved by about twice compared with the result of 2.8×10^{-6} for $\lambda_{({}^1S_0\rightarrow 3\gamma)}/\lambda_{({}^1S_0\rightarrow 2\gamma)}$ obtained in Ref. [9].

In summary, we get the most stringent upper limit of the C-violating process in the pure leptonic system. Comparing with the hadron decay processes, the limit is less stringent than that of 3.1×10^{-8} for $\lambda_{\pi^0\to3\gamma}/\lambda_{\text{total}}$ [12] while it is more stringent than that of 5×10^{-6} for $\lambda_{\eta\to\pi^0\mu^+\mu^-}/\lambda_{\text{total}}$ [13]. Finally, we say that the C invariance holds in the pure leptonic system up to the experimental sensitivity.

ACKNOWLEDGMENTS

We wish to thank Dr. S. Nagayama and S. Adachi for providing the simulation programs. This research was partially supported by a Grant in Aid for Scientific Research from the Ministry of Education, Science, Sports and Culture of Japan.

[1] S. Berko and H. N. Pendleton, Annu. Rev. Nucl. Part. Sci. **30**, 543 (1980), and references therein.
[2] A. Rich, Rev. Mod. Phys. **53**, 127 (1981), and references therein.
[3] J. S. Nico *et al.*, Phys. Rev. Lett. **65**, 1344 (1990), and references therein.
[4] S. Adachi *et al.*, Phys. Rev. Lett. **65**, 2634 (1990); Phys. Rev. A **49**, 3201 (1994).
[5] H. von Busch *et al.*, Phys. Lett. B **325**, 300 (1994).
[6] T. Matsumoto *et al.*, Phys. Rev. A **54**, 1947 (1996) .
[7] W. Bernreuther *et al.*, Z. Phys. C **41**, 143 (1988).
[8] M. Skalsey and J. Van House, Phys. Rev. Lett. **67**, 1993 (1991).
[9] A. P. Mills and S. Berko, Phys. Rev. Lett. **18**, 420 (1967).
[10] H. S. Mani and A. Rich, Phys. Rev. D **4**, 122 (1971).
[11] K. Marko and A. Rich, Phys. Rev. Lett. **33**, 980 (1974).
[12] J. McDonough, V. L. Highland, and W. K. McFarlane, Phys. Rev. D **38**, 2121 (1988).
[13] R. I. Dzhelyadin *et al.*, Phys. Lett. **105B**, 239 (1981).
[14] W. R. Nelson, H. Hirayama, and D. W. O. Rogers, SLAC Report No. 265, 1985 (unpublished).
[15] T. Ishikawa *et al.*, KEK Report No. 92-19, 1993 (unpublished).
[16] S. Kawabata, Comput. Phys. Commun. **41**, 127 (1986).
[17] C. Montanet *et al.*, Particle Data Group, Phys. Rev. D **50**, 1281 (1994).